World Scientific
www.worldscientific.com

SYNTHESIS AND CHARACTERIZATION OF AU NANOPARTICLES/REDUCED GRAPHENE OXIDE NANOCOMPOSITE: A FACILE AND ECO-FRIENDLY APPROACH

MEILING ZOU, HAN ZHU, PAN WANG and SHIYONG BAO

Faculty of Materials and Textiles
Zhejiang Sci-Tech University
310018 HangZhou, P. R. China

MINGLIANG DU* and MING ZHANG

Key Laboratory of Advanced Textile Materials and Manufacturing Technology
Zhejiang Sci-Tech University
Ministry of Education
Hangzhou 310018, P. R. China
*du@zstu.edu.cn

In this paper, epigallocatechin gallate (EGCG) was used as a green reductant both for the fabrication of soluble reduced graphene oxide (rGO) and the synthesis of Au nanoparticles/rGO nanocomposite. Fourier transform infrared (FTIR) spectra confirmed the efficient removal of the oxygen-containing groups in graphene oxide (GO) through the reduction act of EGCG. Au nanoparticles (AuNPs) were anchored onto the rGO sheets by heating the mixed solution of rGO and chloroauric acid at 65°C using EGCG as reductant. Transmission electron microscopy (TEM), atomic force microscope (AFM) and X-ray photoelectron spectroscopy (XPS) were employed to characterize the resulting nanocomposite. Due to the chelating effect of polyhydroxy EGCG, AuNPs with diameters of ~20–50 nm were stably decorated onto both sides of the rGO sheets. Because this reduction method avoids the use of toxic reagents, AuNPs/rGO nanocomposite would be eco-friendly, and it might be useful not only for electronic devices but also for biocompatible materials in the future applications.

Keywords: Epigallocatechin gallate; soluble reduced graphene oxide; Au nanoparticles/reduced graphene oxide.

1. Introduction

Graphene sheets are of great significance in fundamental and applied science for their exceptional electronic, mechanical, plasma processes and thermal properties,[1–6] leading to the development of graphene-based strain sensors,[7] molecular resolution sensor,[8] electromechanical devices[9–11] and surface enhanced Raman scattering substrates.[12] Currently, there is a great interest in functioning the graphene by chemical modification or doping nanosized noble

metals to enhance its electrical, sensing and interfacial properties.[13–16] Decorating reduced graphene oxide (rGO) with Au nanoparticles (AuNPs) is a promising area for various applications, ranging from heterogeneous catalyst,[17] electrochemical sensor[18] to biochemical sensing application.[19]

Various methods have been reported for the synthesis of AuNPs/rGO nanocomposite, including solution chemical approach,[20–22] electrochemical deposition of AuNPs onto rGO sheets,[23] microwave irradiation,[24] ultrasonication,[25] etc.

Chemical reduction of graphene oxide (GO) is considered to be one of the most eco-accessible and easy-controllable methods for preparing rGO on a large scale. The chemical reduction of GO typically involves highly toxic reducing agents which are harmful to human health and environment, and complicated surface modification is often needed to avoid aggregation of the rGO during reduction process.[26,27] Typically, solution chemistry approach, toxic reducing agent $NaBH_4$ and hydrazine hydrate are always widely used for the reduction of $HAuCl_4$ and GO sheets.[28,29] What is more, after reducing approach, rGO could not be dissolved in water again because of the removal of hydrophilic groups. To overcome these disadvantages, it is quite significant to find an efficient, green, eco-friendly way for the preparation of water-soluble AuNPs/rGO nanocomposite.

Epigallocatechin gallate (EGCG) is an environment-friendly reducing agent used in redox reaction recently, and it has been used as a green reducing agent for the synthesis of many noble nanoparticles in our previous research.[30,31] In this work, rGO was considered as a support for the deposition of AuNPs. We presented the synthesis and characterization of AuNPs/rGO nanocomposite by using a simple and green synthesis method, based on the use of EGCG as a multiple role-play reagent, reductant and stabilizer, for the preparation of rGO and AuNPs. Uniform and extensive cover of AuNPs on rGO sheets can be obtained.

2. Experimental Section

2.1. *Materials*

Graphite powder (99.9995%) was obtained from Alfa-aesar Co., Ltd. Concentrated sulfuric acid (H_2SO_4, 95–98%), potassium permanganate ($KMnO_4$), hydrogen peroxide (H_2O_2, 30 wt.%), concentrated hydrochloric acid (HCl, 0.1 mol/L) and Chloroauric acid ($HAuCl_4 \cdot 4H_2O$, 99.9%) were purchased from Aladdin Chemistry Co., Ltd. EGCG was purchased from Xuancheng BaiCao Plant Industry and Trade Company and used as received without further purification. Deionized water was used for all solution preparations.

2.2. *Methods*

2.2.1. *Synthesis of EGCG–rGO*

GO nanosheets was synthesized based on Hummers method.[32] Hu's approach for the synthesis of GO is adopted through oxidizing the graphite powder in a mixture of concentrated sulfuric acid and $KMnO_4$.[26] For the preparation of rGO, in a typical procedure, GO aqueous solution (1 mg/mL) was prepared by sonication of 150 mg GO nanosheets in deionized water, and the GO dispersion was brownish yellow [see Fig. 1(a)], then 300 mg EGCG (200 wt.% relative to GO) was added. The mixture was maintained at 80°C under vigorous stirring for 6 h. After being cooled to room temperature, the resulting mixture was centrifuged at 8000 rpm for 20 min and washed with ultrapure water five times to remove the residual EGCG. Finally, the product was dispersed in 150 mL ultrapure water and kept at room temperature.

2.2.2. *Fabrication of rGO–AuNPs*

Typically, 5 mL $HAuCl_4$ (10 mmol/L) was dropped tardily to 50 mL rGO solution and kept stirring for 30 min, and then the mixture was heated to 65°C. rGO — AuNPs was prepared by adding 5 mL EGCG (0.5 mg/mL) solution to the mixture
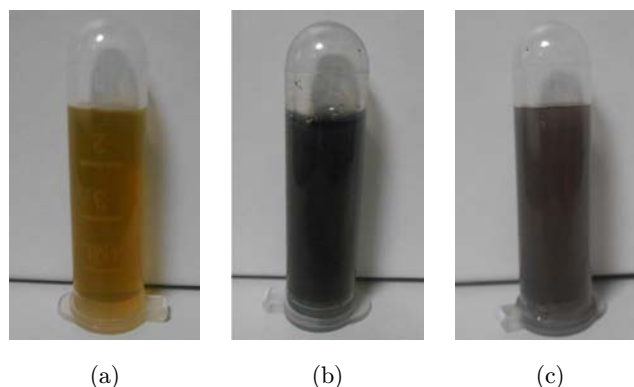

(a)   (b)   (c)

Fig. 1.   Typical pictures of GO (a), brownish yellow, rGO (b), black and AuNPs/rGO (c), atropurpureus (color online).
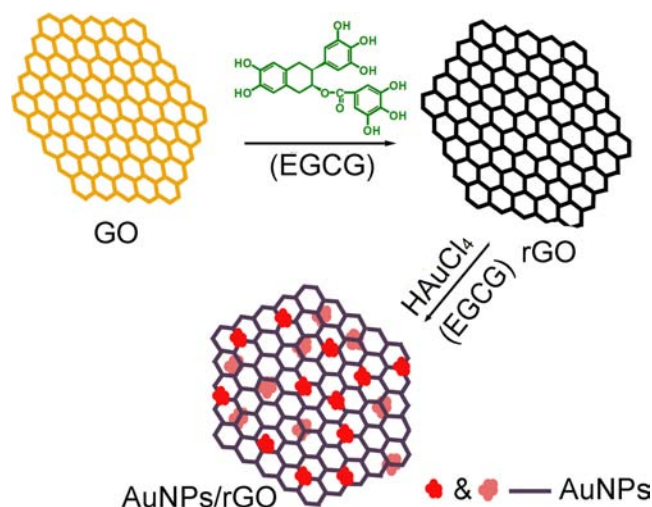
Fig. 2. Fabrication procedure of AuNPs/rGO (color online).

followed by vigorous stirring. The addition of EGCG solution was controlled drop-wise and the color of the mixture changed from black to atropurpureus [see Figs. 1(b) and 1(c)]. After 2 h, the mixture was centrifuged at 8000 rpm for 20 min and washed with ultrapure water for five times. Ultimately, the product was dispersed in 50 mL ultrapure water at room temperature. The whole fabrication procedure of AuNPs/rGO is presented in Fig. 2.

2.3. *Characterization*

Fourier transform infrared (FTIR) spectra were recorded on a Nicolet 5700 spectrophotometer. Transmission electron microscopy (TEM) characterization was performed on a JEOL JEM-2100 electron microscope operating at 200 kV. Powder X-ray diffraction (XRD) patterns were collected using a SIEMENS Diffractometer D5000 X-ray diffractometer using a CuKα radiation source at 35 kV, with a scan rate of $0.02 \, \mathrm{s}^{-1}$ in the 2θ range of 3–90°. Atomic force microscopy (AFM) images were obtained using a digital Nanoscope IIIa Atomic Force Microscope in tapping mode. X-ray photoelectron spectra of AuNPs/rGO was recorded using an X-ray photoelectron spectrometer (Kratos Axis Ultra DLD) with an aluminum (mono) Kα source.

3. Results and Discussion

The AFM image in Fig. 3(a) shows the morphology of as-prepared GO, where the cross-sectional view indicates that the average thickness of GO sheets is about 1 nm, suggesting that the GO sheets are fully exfoliated. Figures 3(b) and 3(c) shows the typical TEM image of the prepared GO and rGO, respectively. It can be seen that, after reduced by EGCG, the morphology of the rGO does not have obvious
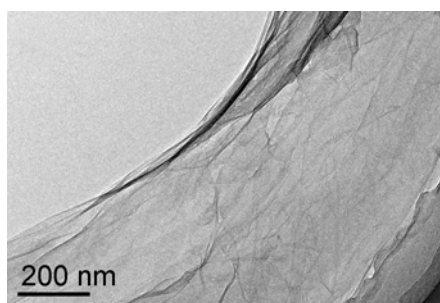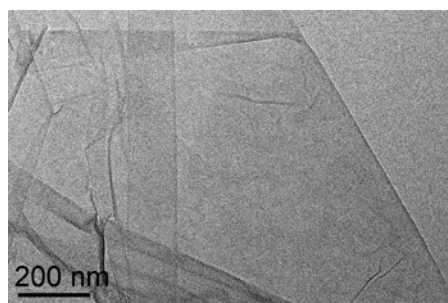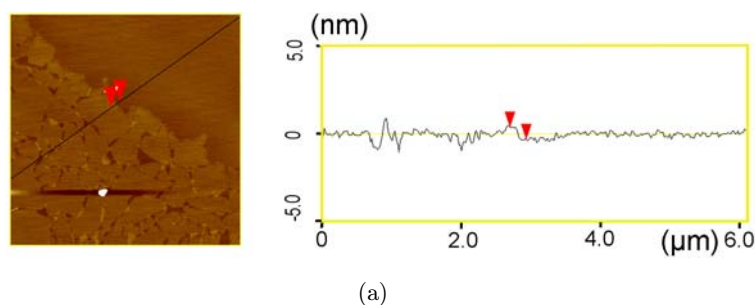

(a)

(b)

(c)

Fig. 3.   AFM image of GO (a) and TEM images of GO (b) and rGO (c) (color online).
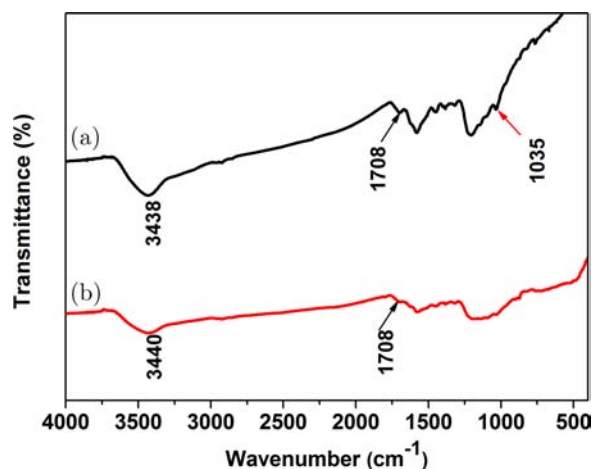
Fig. 4. FTIR spectra of GO (a) and rGO (b) (color online).

changes. And the rGO remains as an intact piece of sheet.

FTIR technique was utilized to characterize the chemical changes of GO after reduction process. As shown in Fig. 4, the peaks from the range of $900\,\mathrm{cm}^{-1}$ to $1500\,\mathrm{cm}^{-1}$ can be ascribed to the functional groups (epoxy groups and carboxyl groups) of GO.[33] Curve a and b show an evident broad absorption peak at $3438\,\mathrm{cm}^{-1}$ and $3440\,\mathrm{cm}^{-1}$ respectively, which are assigned to the O–H stretching vibration of hydroxyls. After the reduction, the

peaks at $1708\,\mathrm{cm}^{-1}$ assigned to carboxyl groups and $1055\,\mathrm{cm}^{-1}$ assigned to epoxy groups are decreased significantly, clearly indicating the removal of oxygen containing groups of GO. In addition, the aqueous GO is light brown, after reduction, it turned to black (as shown in Fig. 1), suggesting the successful reduction of GO.

Besides, according to some reductants that have the common characteristics to EGCG, such as tannic acid and tea polyphenols that have been reported in the literature,[34,35] we proposed a procedure for the preparation of rGO. However, most of the epoxide groups are believed to be removed more easily than hydroxyl and carboxyl during the reduction, therefore, the mechanism of epoxy groups on GO that converted to carboxyl groups may proceed via a two-step SN_2 nucleophilic reaction and elimination with the release of H_2O,[37] which is demonstrated in Fig. 5. As is well known, that GO can be easily dissolved in water solution is mainly caused by the oxygen-containing groups. Usually, the removal of surface oxygen-containing groups in GO will lead to irreversible aggregation, therefore, a stabilizer is always needed to prevent or reduce the aggregation. According to previous literatures,[35] the interaction between stabilizer and rGO were considered to be π–π and van der Waals interactions. While the
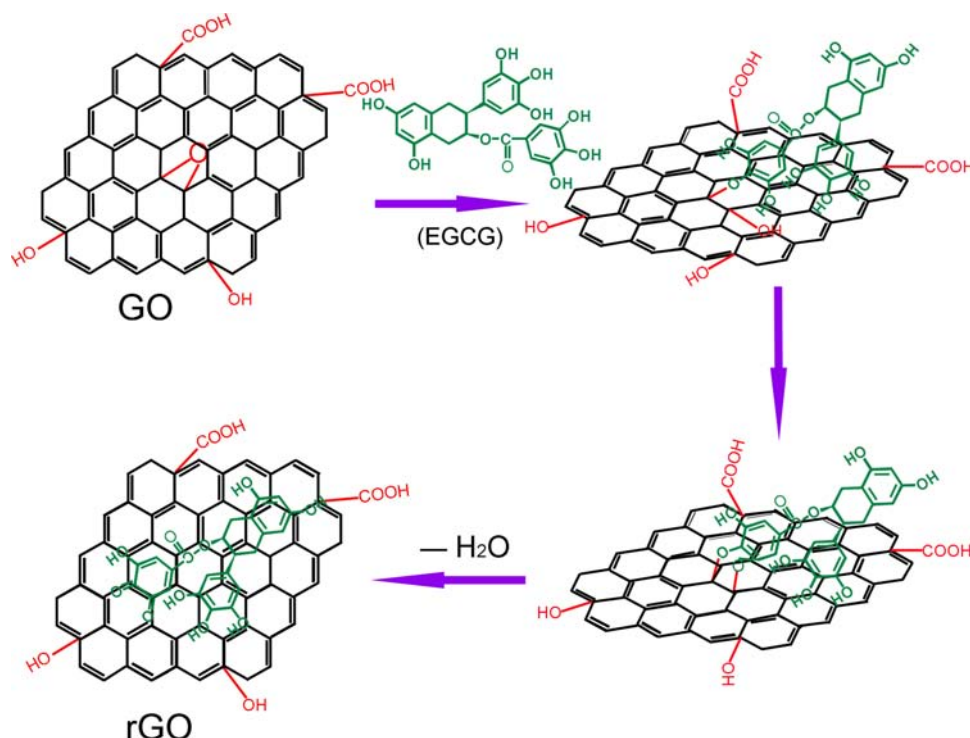

Fig. 5. Proposed reaction pathway for the chemical reduction of GO by EGCG (color online).
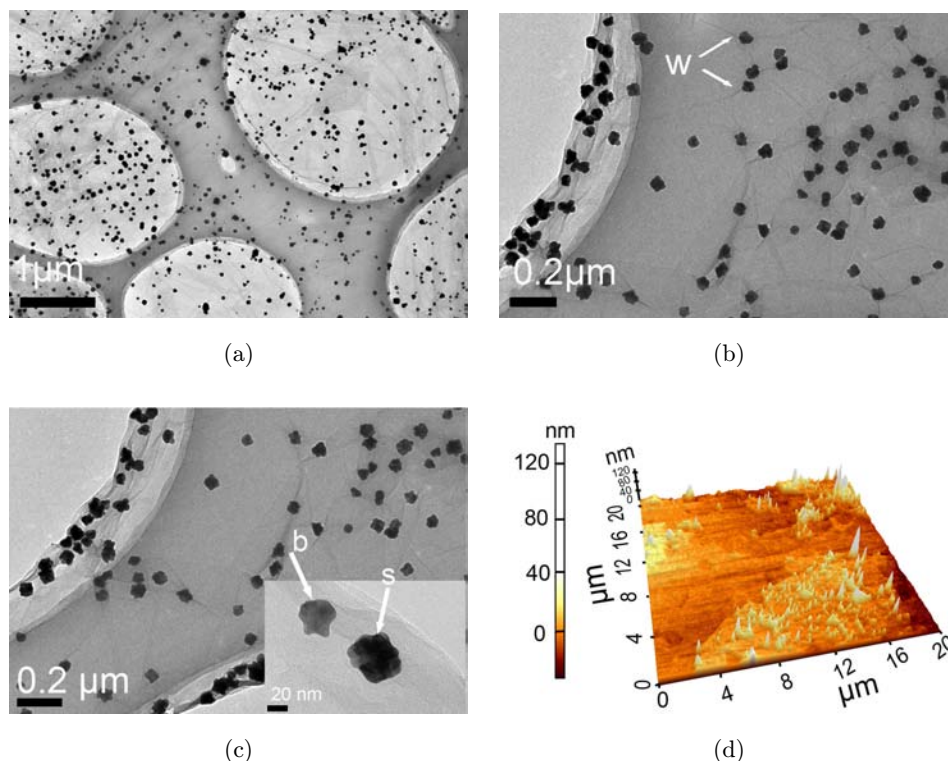
Fig. 6. TEM images of AuNPs/rGO nanocomposite under various magnifications (a), (b) and (c); AFM image of AuNPs/rGO (d) (color online).

interaction between oxidized EGCG and rGO is believed to mainly be π–π interaction. Finally, due to the strong interactions between rGO and O–EGCG that avoids the aggregates of rGO sheets, the colloidal solution exhibits good stability and solubility in water without any addition of surfactant.

Figures 6(a)–6(c) display the TEM images of AuNPs/rGO nanocomposite under various magnifications. It is observed from Fig. 6(a) that there is a homogeneous and dense coverage of AuNPs on the surface of rGO sheets and the diameters of AuNPs vary from 20 nm to 50 nm. As shown in Figs. 6(b) and 6(c), the AuNPs/rGO displays the characteristic of wrinkled morphology (darker lines, labeled as "W"). On one hand, the wrinkles are caused by the surface chemical property of rGO itself, on the other hand, the loading of AuNPs can also lead rGO to wrinkle, accordingly, flower-like AuNPs are apt to form around the wrinkles. Besides, it is believed that Au ions can nucleate on both sides of the rGO sheets when exposed to the solvent, therefore, it can be seen from the inset of Fig. 6(c) that the AuNPs appearing darker (labeled as "s") were probably attached to the surface of rGO and the others labeled as "b" were on the back of the sheets.

Because of the shielding effect of rGO sheets, the AuNPs that on the back of the sheets were given lesser average surface-electron density, resulting in lighter appearance than the surface AuNPs. Figure 6(d) shows the AFM image of AuNPs/rGO in three dimensions, and the small white acuminations represent AuNPs. As a result, rGO supported nanocomposite is prepared successfully with AuNPs anchored onto both sides of the sheets.

To further characterize the deposition of the AuNPs on the surface of rGO, the XRD patterns of the GO, rGO and AuNPs/rGO were collected as shown in Fig. 7. The as-prepared GO shows a characterized peak at $2\theta = 9.6°$, corresponding to an interlayer d-spacing of 0.92 nm. Compared to GO, the rGO shows a peak centered at 4.9°, indicating that the interlayer distance increases to 2.1 nm. The expanded interlayer distance can result from the attachment of EGCG molecules among the GO layers. Besides, another broad peak is located at 24.5°, implying a smaller interlayer distance of 0.35 nm, which can resulted from the restack of graphene layers. The AuNPs/rGO exhibits the typical peaks of AuNPs at 2θ value of 38.2°, 44.5°, 64.6°, 77.8°, 82.0°, matching to Au (111), Au (200),
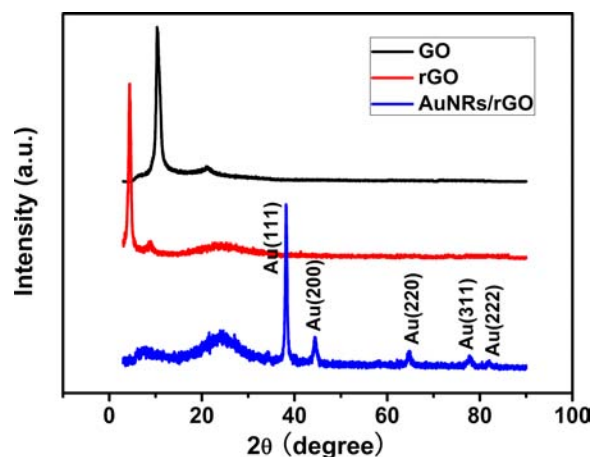
Fig. 7.   Powder XRD patterns of GO, rGO and AuNPs/rGO (color online).

Fig. 9.   XPS survey scans of Au 4f region of AuNPs/rGO.

Au (220), Au (311) and Au (222) crystal face, respectively, which suggests the formation of face-centered cubic AuNPs.

The binding of rGO with AuNPs was also confirmed by UV-Vis spectroscopy (see Fig. 8). The optical absorption of GO and rGO in the visible light region cannot be observed. The AuNPs/rGO nanocomposite shows an obvious peak at 560 nm, which can result from the surface plasmon absorption of AuNPs, compared with that of rGO, which further indicates that the AuNPs are loaded on the surface of GO sheets.

The chemical state of AuNPs in the nanocomposite was identified by XPS measurement and the resultant Au 4f spectrum is shown in Fig. 9. As observed in Fig. 9, the intense doublets that emerged at 84.42 eV and 88.02 eV correspond well
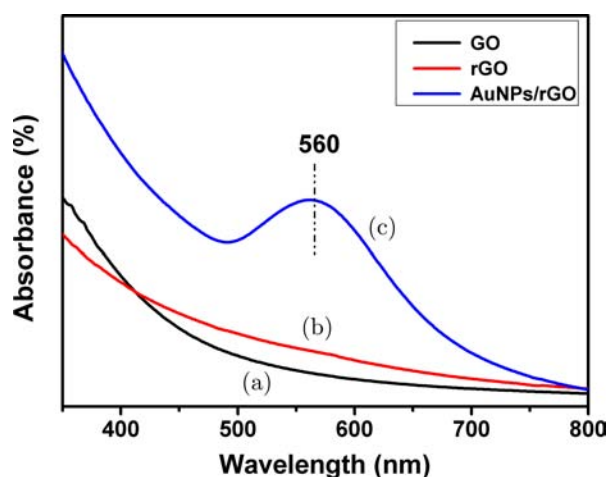
with Au $4f_7$ and Au $4f_5$ binding energies, respectively. Compared with zero valent Au^0 (84.0 eV and 87.7 eV), there is a shift of about 0.42 eV and 0.95 eV, respectively. Above changes of the binding energy indicate the different chemical environment between the AuNPs in the composite and Au^0.[36] The relatively higher binding energy can be attributed to the interaction of AuNPs with EGCG molecules. The surface Au atoms of AuNPs exposed to the surrounding stabilizer with passive charges would donate electron to stabilizer, causing a positive shift in Au 4f core level. As discussed above, due to the chelating interactions of Au ions with EGCG during the synthesis, EGCG serves as a reducer as well as a stabilizer. All the above observations suggest the successful decoration of AuNPs onto rGO sheets. Most important, due to the synergistic effect of polyhydroxy EGCG, AuNPs/rGO can be homodispersed in aqueous solution stably.

4.   Conclusions

In this work, the synthesis method of AuNPs/rGO nanocomposite was reported and a systematical characterization of the nanocomposite material was presented. The method is simple, green, low cost, which can be easily realized under mild conditions. Above all, the water soluble rGO was prepared via a chemical reduction process, the strong interactions between rGO and the oxidized EGCG enabled the good dispersion of rGO in aqueous solution. Based on the prepared rGO, AuNPs with the diameter of ~20–50 nm were decorated on both sides of the rGO sheets, as a result, the AuNPs/rGO nanocomposite

Fig. 8.   UV-Vis spectra of GO (a), rGO (b) and AuNPs/rGO (c) (color online).

material that can be well dispersed in water was obtained. Therefore, this nanocomposite prepared via the green, facile strategy reported here would have many potential applications, such as electronic devices and biocompatible materials.

Acknowledgments

References

1. A. K. Geim and K. S. Novoselov, *Nat. Mater.* **6**, 183 (2007).
2. S. Ghosh, I. Calizo, D. Teweldebrhan *et al.*, *Appl. Phys. Lett.* **92**, 151911 (2008).
3. S. H. Hur and J. Park, *Asia-Pac. J. Chem. Eng.* **8**, 218 (2013).
4. P. Blake, P. D. Brimicombe, R. R. Nair *et al.*, *Nano Lett.* **8**, 1704 (2008).
5. C. W. Twombly, J. S. Evans, I. I. Smalyukh *et al.*, *Opt. Express* **21**, 1324 (2013).
6. Z. Bo, Y. Yang, J. H. Chen *et al.*, *Nanoscale* **5**, 5180 (2013).
7. Y. Wang, R. Yang, Z. W. Shi *et al.*, *Acs Nano* **5**, 3645 (2011).
8. O. K. Kwon, K. S. Kim, J. Park *et al.*, *Comput. Mater. Sci.* **67**, 329 (2013).
9. Y. U. Jung, S. Oh, S. Choa *et al.*, *Curr. Appl. Phys.* **13**, 1331 (2013).
10. J. J. Liang, L. Huang, N. Li *et al.*, *Acs Nano* **6**, 4508 (2012).
11. N. Al-Aqtash, H. Li, L. Wang *et al.*, *Carbon* **51**, 102 (2013).
12. S. J. He, K. K. Liu, S. Su *et al.*, *Anal. Chem.* **84**, 4622 (2012).
13. T. Wu, L. Zhang, J. P. Gao *et al.*, *J. Mater. Chem. A* **1**, 7384 (2013).
14. K. Jasuja, J. Linn, S. Melton *et al.*, *Phys. Chem. Lett.* **1**, 1853 (2010).
15. A. Guimont, E. Beyou, P. Alcouffe *et al.*, *Polymer* **54**, 4830 (2013).
16. V. J. Surya, K. Iyakutti, H. Mizuseki *et al.*, *Comput. Mater. Sci.* **65**, 144 (2012).
17. H. J. Yin, H. J. Tang, D. Wang *et al.*, *Acs Nano* **6**, 8288 (2012).
18. Y. Q. Hu, Z. H. Xue, H. X. He *et al.*, *Biosens. Bioelectron.* **47**, 45 (2013).
19. L. Li, H. M. Lu and L. Deng, *Talanta* **113**, 1 (2013).
20. J. Gao, F. Liu, Y. L. Liu *et al.*, *Chem. Mater.* **22**, 2213 (2010).
21. C. Z. Zhu, S. J. Guo, Y. X. Fang *et al.*, *Acs Nano* **4**, 2429 (2010).
22. D. R. Dreyer, R. S. Ruoff and C. W. Bielawski, *Angew. Chem. Int. Ed.* **49**, 9336 (2010).
23. C. P. Fu, Y. F. Kuang, Z. Y. Huang *et al.*, *Chem. Phys. Lett.* **499**, 250 (2010).
24. K. Jasuja, J. Linn, S. Melton *et al.*, *J. Phys. Chem. Lett.* **1**, 1853 (2010).
25. N. Y. Cheng, J. Q. Tian, Q. Liu *et al.*, *ACS Appl. Mater. Interfaces* **5**, 6815 (2013).
26. C. F. Hu, J. H. Rong, J. H. Cui *et al.*, *Carbon* **51**, 255 (2013).
27. Y. J. Zhang, W. B. Hu, B. Li *et al.*, *Nanotechnology* **22**, 345601 (2011).
28. X. Y. Qi, K. Pu, X. Z. Zhou *et al.*, *Small* **6**, 663 (2010).
29. Y. C. Si and E. T. Samulski, *Nano Lett.* **8**, 1679 (2008).
30. H. Zhu, M. L. Du, M. Zhang *et al.*, *Sens. Actuators B* **185**, 608 (2013).
31. P. Wang, H. Zhu, S. Y. Bao *et al.*, *J. Phys. D: Appl. Phys.* **46**, 345303 (2013).
32. W. S. Hummers and R. E. Offeman, *J. Am. Chem. Soc.* **80**, 1339 (1958).
33. X. Liu, X. Y. Wang, P. Y. He *et al.*, *J. Solid State Electrochem.* **16**, 3929 (2012).
34. Y. Wang, Z. X. Shi and J. Yin, *ACS Appl. Mater. Interfaces* **3**, 1127 (2011).
35. Y. D. Lei, Z. H. Tang, R. J. Liao *et al.*, *Green Chem.* **13**, 1655 (2011).
36. H. Zhu, M. L. Du, M. L. Zou *et al.*, *J. Mater. Chem.* **22**, 9301 (2012).
37. R. J. Liao, Z. H. Tang, Y. D. Lei *et al.*, *J. Phys. Chem. C* **115**, 20740 (2011).